THERMAL AND AUSTENITIC THERMOCHEMICAL SURFACE HARDENING OF STEEL

T. Ericsson

[1]*Department of Mechanical Engineering, Institute of Technology, Linköping University, Linköping, Sweden*

ABSTRACT

An overview is given of the recent development of induction, laser and electron beam hardening and of carburizing/ carbonitriding of steel. New trends regarding the technology are mentioned but the emphasis is on progress in the transformation of steel and the resulting properties. A fairly complete review is given of computer models for the hardening process and for strength predictions. Finally the advantages and drawbacks of the hardening methods treated are listed and the preferred applications indicated.

KEYWORDS

Induction hardening laser hardening; electron beam hardening; carburizing; carbonitriding; case hardening; austenite; martensite; residual stress.

INTRODUCTION

Very often the surface is the most strained part of a component. The stresses are at a maximum at the surface during bending and it is the surface that is exposed to wear and corrosion. Therefore it is natural that a number of methods to strengthen the surface have been developed. In this overview paper surface hardening of steel will be treated. A brief description of the processes from technological and metallurgical aspects as well as microstructures and properties will be given.

Modern classifications distinguish between thermal and thermochemical treatments. The thermal treatments that will be covered here are induction, laser and electron beam hardening; and the austenitic thermochemical treatments, carburizing and carbonitriding.

A rapid development has occurred in the last decade involving new heat sources and new gas atmospheres. This is well covered in a series of conference proceedings (Metals Society, 1972, 1974, 1977, 1980, 1982, 1984, 1985). The new edition of the Metals Handbook (ASM, 1981) gives up-to-date descriptions of various surface hardening processes. Induction hardening and carburizing/carbonitriding are also extensively treated in a recent book by Thelning (1984).

Induction Hardening

In induction hardening the surface of the steel is heated into the austenitic state by eddy currents flowing in a coil surrounding the surface. The heating time is normally quite short, less than half a minute. The steel is subjected to forced cooling by spraying a water solution onto surface. The austenite then transforms to martensite giving the component a hard surface. The interest in induction hardening is growing because it is a fast and clean method well suited to in-line applications. The development of induction heating systems has been from motor generator equipment (low frequencies) or vacuum oscillator tube systems (high frequencies) toward solid state power sources and control (Bobart, 1982). The power output is usually between 50 and 100 kW. Automatic handling has also become more common (Reinke and Gowan, 1978). One distinguishes between single shot hardening and progressive (scanning) hardening. In single-shot hardening the induction coil and cooling ring are as long as the workpiece and thus harden the whole area at the same time. Progressive hardening uses a short coil and the long workpiece is fed through the coil and quenching ring. The choice of either principle is dependent on the size and shape of the component to be hardened. It has been claimed that single-shot hardening is suitable for fast automated systems (Reinke and Gowan, 1978).

Mathematical models have recently been developed by Melander (1982, 1983, 1984a, 1984b) to describe induction hardening with the specific objective of calculating the resulting residual stresses. The description gives a good understanding of the physical principles involved. Alternating current is applied to the induction coil which gives rise to a magnetic field and this field induces eddy currents in the workpiece. Eddy current losses heat up the piece. The depth of penetration δ (skin depth) is mainly determined by the frequency f:

$$\delta = \sqrt{(\rho_r/\mu\pi f)}$$

where ρ_r is the resistivity and μ the permeability; both are temperature dependent.

The interior of the material is heated by conduction from the skin layer.

Typical hardened depths for various frequencies are shown in Table 1 (Bobart, 1982). It is obvious that quite a wide range of depth can be obtained.

TABLE 1 Induction Heating Hardened Depths

Frequency	Typical hardened depth [mm (inches)]
450 kHz	less than 1.59 (1/16)
10 kHz	1.59 to 3.18 (1/16 to 1/8)
3 kHz	3.18 to 6.35 (1/8 to 1/4)
1 kHz	6.35 to 9.53 (1/4 to 3/8)
180 Hz	9.53 (3/8) to full hardenability depth
60 Hz	full hardenability depth

The heating time is very short and is directly followed by quenching. Therefore the surface layer is in the austenitic state for only a few seconds. Figure 1 shows experimentally determined temperature curves and calculated curves for single shot hardening of a 40 mm diameter steel bar at three different depths below the surface (Melander, 1983; Melander et al., 1984).

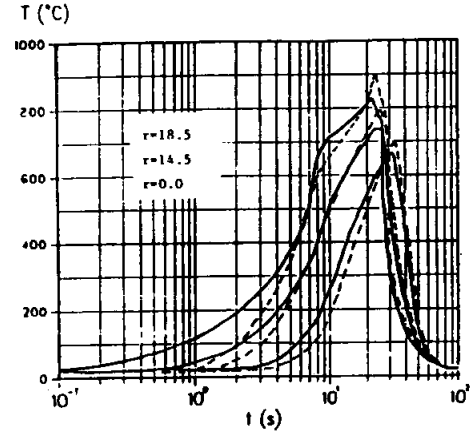

Fig. 1. Experimentally determined temperature curves (dashed lines) and calculated temperature curves (full lines) at different radii (Melander et al., 1984).

One can notice the turn-off of power and the onset of the cooling shower.

To get a high enough degree of hardness (30-50 HRC), steels for induction hardening normally contain more than 0.3% C. To avoid hardening cracks the C-content is limited to 0.5% C. With special care steels with higher C-contents can be induction hardened as well as cast irons. In the virgin material the carbon is present in carbides. Finely distributed carbides give more complete carbide dissolution during the short heating time. Therefore quenched and tempered or normalized steels are preferred to fully annealed steels. To judge the induction hardening response not only isothermal cooling (ITc) or continuous cooling diagrams (CCT) are useful but also isothermal heating diagrams (ITh) or continuous heating diagrams (CHT). Examples are shown in Figs. 2, 3. Notice that a shorter austenitizing time in Fig. 3 moves the pearlite and bainite noses to the left, i.e. decreases the hardenability due to incomplete carbide dissolution. A higher austenitizing temperature ($\sim$50°C) than for conventional hardening has to be used to austenitize the steel in a short time, see Fig. 2. ITh diagrams are not so easily available as ITc ones, but at least one comprehensive source exists (Atlas zur Warmebehandlung der Stahle, 1973).

The progress of the induction hardening has been studied by computer calculations (Melander, 1982; Melander et al., 1984; Ericsson and Hildenwall, 1982). Figure 4 shows the volume fraction plotted against time for the same case as in Fig. 1, i.e. single-shot hardening. Progressive induction hardening has also been analysed by Melander et al. (1984).

After 7 s austenite starts to form which causes a constant temperature for a while (Fig. 1) due to absorption of heat in transformation. After about 20 s the surface layer is completely austenitic. The austenite starts to transform to martensite when the water cooling sets in after about 28 s. The final phase distribution is shown in Fig. 5. It is martensitic down to 1 mm depth then partially martensitic and partially pearlitic to about 4 mm depth. (No distinction is made between the original Q&T structure and the newly formed pearlite).

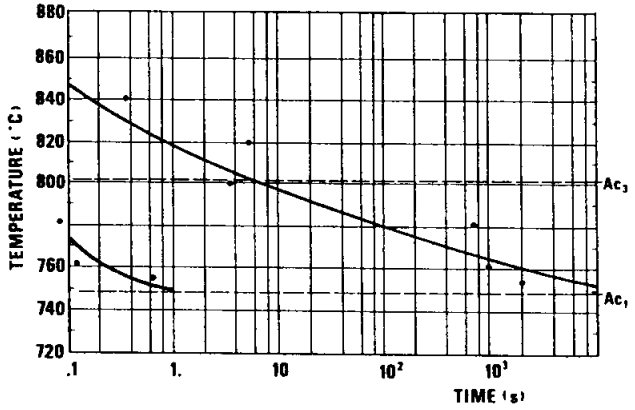

Fig. 2. Experimentally determined ITh-diagram for steel SS 2244. Heating rate ∿1000 °C s^{-1}

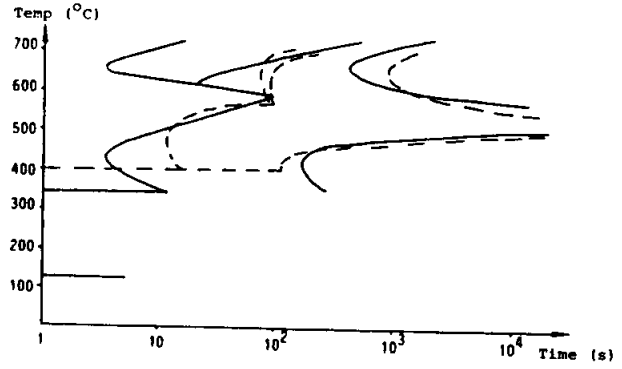

Fig. 3. Experimentally determined ITc-diagrams for a short austenite holding time (full lines) and a standard diagram (dashed lines). The same steel is used as for Fig. 2 SS 2244 ≈ AISI 4140

It is also illustrative to follow the residual stress development in the cylinder, (Fig. 6). After 5 s the stress is compressive in the surface due to the temperature gradient. After 10.7 s the stress is less compressive due to the added effect of the formation of more dense austenite. The austenitic area is at a maximum after 22 s just before the cooling. The yield stress is low and therefore the austenitic layer is almost stress-free. After 34.5 s martensite has started to form shifting the surface stress in the compressive direction and causing a compensating tensile stress for radii between 11 and 18 mm. Finally compressive stress to a depth of 4 mm is obtained.

Typical hardness profiles obtained, as well as microstructures, are reproduced in a recent book (Thelning, 1984). The hardness gradient is usually very steep. Just below the hardened surface the hardness has a minimum when the

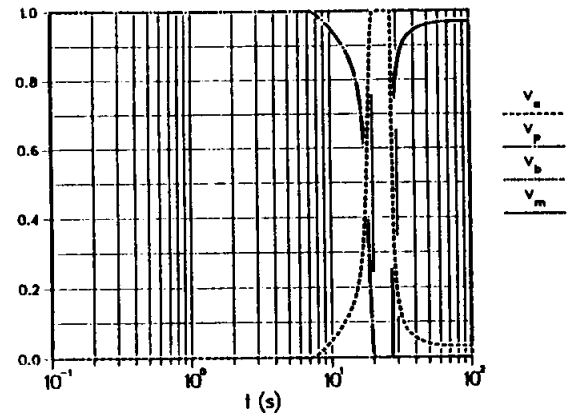

Fig. 4. The calculated phase composition in volume percentages as function of time at the outer surface (Melander et al., 1984)

original structure is Q&T martensite. This is due to annealing of the prior structure. The hardness dip coincides approximately with the tensile residual stress peak that can appear, see Fig. 6. So the layer below the hardened zone may be a weak zone in fatigue.

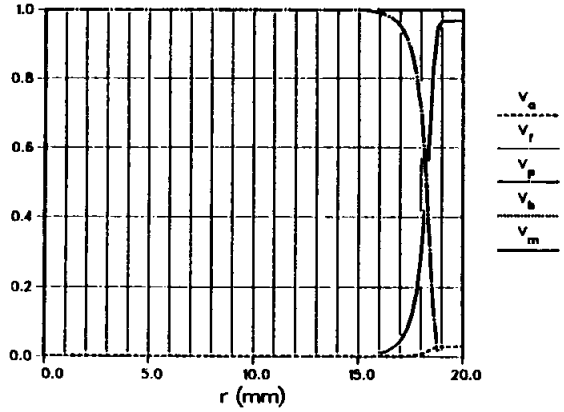

Fig. 5. The calculated phase composition in volume percentages as a function of the radius after finished hardening. V_a = austenite, V_f = ferrite, V_p = pearlite, V_b = bainite, V_m = martensite. (Melander et al., 1984).

Induction hardening is used to improve the fatigue and wear properties of steel. The wear resistance is mainly dependent on the hardness of the case which is determined by the carbon content of the steel. The presence of undissolved carbide can enhance the wear resistance further.

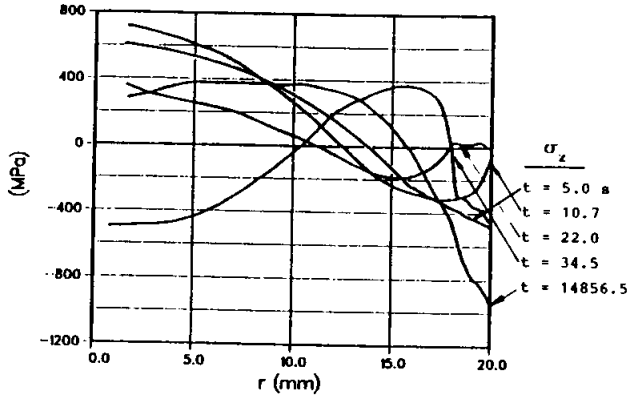

Fig. 6. The calculated stress as a function of radius at various times (Melander et al., 1984).

Like all surface hardening procedures, induction hardening is mainly effective against fatigue in bending, torsion and rolling contact when the strength of the core is of less importance. The standard procedure to predict the required case depth and hardnesses has been well described by Hopkins (1976). The fatigue strength depends mainly on case depth and surface and core hardness. The residual stress profile is also important, especially the magnitude of the surface compressive stress and the pressence of a compensating tensile peak below the case. It should be observed that at the edges of an induction hardened area tensile peaks can also appear (Ishii, 1969).

The short austenitizing times used in induction hardening lead to a fine austenite grain size, which gives the case better toughness properties than would a coarse structure.

LASER HARDENING

Laser hardening has many similarities to induction hardening. Several recent reviews have been published (Hick, 1983; Chatterjee-Fischer, 1984). Laser hardening involves rapid heating and cooling of the surface so that austenite is formed and then quenched to martensite. The heating however occurs in the surface itself and not in a skin. Usually the conditions are such that self quenching is sufficient, i.e. no external cooling medium is required. For hardening applications continuous or pulsed CO_2 lasers are mainly used with power outputs between 1.5 kW and 15 kW., i.e. several orders of magnitude less than for induction hardening. The wave length of the CO_2 laser light is 10.6 μm, i.e. infrared. A clean metallic surface will reflect as much as 95-98% of the infrared light. Therefore the surface is coated to enhance absorption. Suitable materials include graphite, black paint, zinc and manganese phosphates.

The laser light can be focused on the surface and very high incident beam power densities can be achieved. For martensite transformation hardening 10^3-5 x 10^4 W cm^{-2} is used for a few seconds to a fraction of a second, (Fig. 7). It is obvious that with a modest power output only a small area can be heated at a time. Laser hardening is an extreme local hardening process. Surface coverage can vary from 40 to 130 cm^2 min^{-1}.

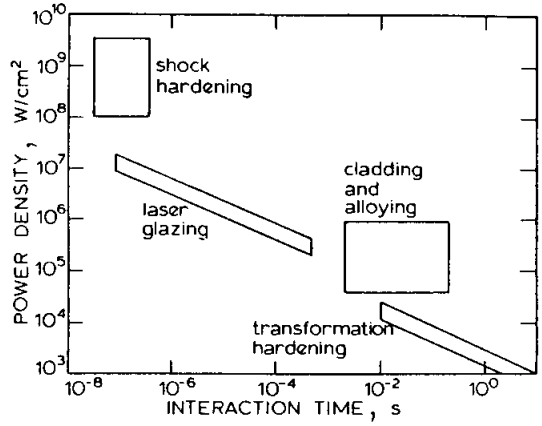

Fig. 7. Operational regimes for the laser heat treating (Hick, 1983).

The beam is manipulated by mirrors and lenses. Typically 1-10 mm wide traces are hardened and the case depths are below 1 mm, but case depths up to 2 mm can be achieved. By help of toric mirrors it is possible to harden a cylindrical outer or inner surface. The diameter is however restricted to small values (10 to 15 mm) due to the limited power output. If one wants to harden larger areas by adding traces beside each other, a problem due to overlap may occur. A subsequent pass will temper an adjacent earlier pass, giving rise to a softer structure. Several computer models have been developed for the calculation of the temperature distribution under a laser beam trace (Godfrey, 1981; Kawasumi, 1981; Courtorey, 1981). An example is shown in Fig. 8a.

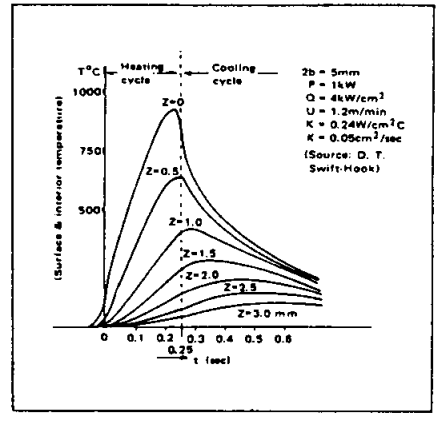

Fig. 8a Calculated temperature-time curves for various depth Z (Kawasumi, 1981).

The temperature distribution measured by thermocouples during a single pass of a laser beam is shown in Fig. 8b. The temperature curve no 3 is measured

0.86 mm below the surface. The beam diameter was 11.5 mm, power 2.4 kW and speed 0.58 m min^{-1}, i.e. the power density was 2.3 kW cm^{-2} and interaction time 1.2 s. The experimental and theoretical curves are comparable as the ratio between the power density and speed is about the same. The temperature rise time is obviously much shorter than in the induction hardening case, see Fig. 1.

Recently a mathematical model for the laser transformation hardening of steel has been presented (Ashby, 1984). An expression is derived for the temperature field under a moving laser beam taking account of the radius of the beam, the beam power and velocity, the thermal conductivity and diffusivity of the material and the absorptivity of the surface. This expression is then combined with diffusion expressions to describe the dissolution of pearlite colonies into austenite and the gradual homogenisation of the carbon content. The results of the calculation are presented in very instructive three-dimensional diagrams with energy density, beam radius and depth on the three axes, (Fig. 9). The diagram shows in which combinations surface melting and hardening occur, and the volume fraction of martensite and the hardness. The hardness is estimated from a linear rule of mixing knowing the hardness of martensite as a function of mean carbon content and of ferrite. The original structure of the 0.6% C steel in Fig. 9 is ferritic-martensitic. A Q&T structure would give different values for the hardened zone.

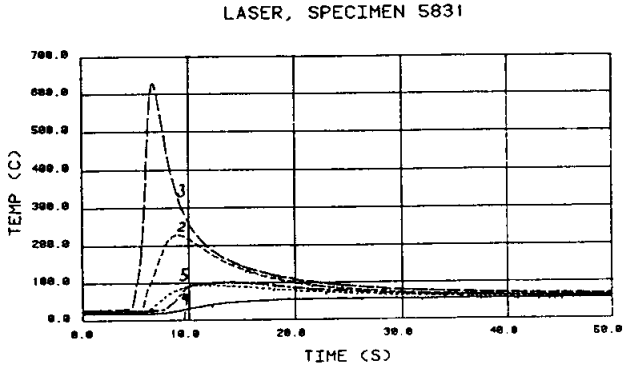

Fig. 8b. Measured temperatures at different depths below the surface. Curve 3 at 0.86 mm below the surface and curve 2 at 4.70 mm.

For the special case of a cylindrical axis moving through a toric mirror the temperature distribution has been calculated (Melander et al., 1984; Kou, 1983). An example is shown in Fig. 10. The input parameters correspond to a power density of 1.5 kW cm^{-2} and an interaction time of 3 s. This is in the lower range for transformation hardening (Hick, 1983). The temperature-time curve is comparable to progressive induction hardening (Melander et al., 1984).

In principle all steels and irons that are hardenable by conventional means can also be laser hardened. Even low carbon steel that normally cannot be induction-hardened can be laser hardened due to the extremely high cooling rates obtainable by self-quenching. The influence of the carbide distribution is even more important than during induction hardening, due to the higher cooling rates normally used. A coarse carbide (pearlite islands) can give rise to martensite islands in a ferritic matrix, described above (Chatterjee-Fischer, 1984; Ashby, 1984)

High retained austenite contents have been reported in the outer layers of

laser hardened medium carbon low alloy steels (Chatterjee-Fischer, 1984; Molian, 1981). The same steels exhibit no retained austenite after induction hardening. The high cooling rate is a likely reason for the retention of austenite (Molian, 1981) although carbon dissolution from an absorbing graphite coating may magnify the effect in the very surface.

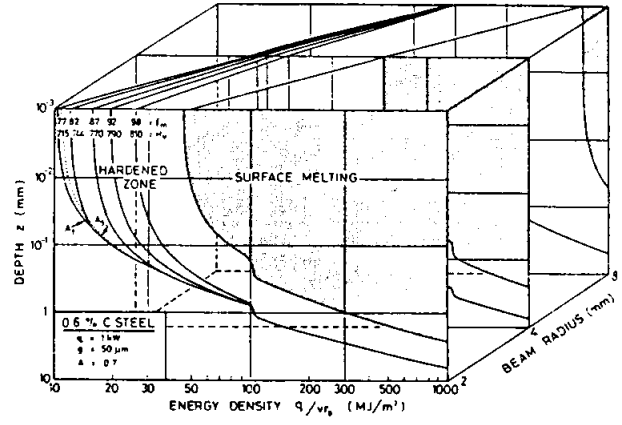

Fig. 9. A diagram describing the laser-processing of an 0.6 wt% C carbon steel (Ashby, 1984).

The hardeness profiles normally show a steep gradient at the case/core boundary. If the core is martensite or bainite tempered at a moderate temperature a softer zone can be found next to the case due to extra tempering as in induction hardening.

Tensile as well as compressive surface residual stresses have been reported after laser hardening by Chatterjee-Fischer (1984). Measurements across a single 8 mm wide pass on 0.4% C carbon steel have shown compressive stresses in the middle 4 mm, compensating tensile stresses in 3 mm wide zone on either side and again compressive stresses further aside.

The laser hardening using a toric mirror mentioned above gave compressive stresses in the hardened case (Table 2).

TABLE 2 Residual Stresses at Different Depths Below the Surface of a Cylinder with 15 mm Diameter for Two Steels Hardened by Laser using a Toric Mirror and Self Quenching

Steel AISI 52100		Steel AISI 4140	
Depth (mm)	Residual stress (MPa)	Depth (mm)	Residual stress (MPa)
0	-320	0	-460
0.03	-320	0.05	-410
0.60	-170	0.62	-220
0.93	-170		

Laser hardening is mainly used to improve wear properties. An often cited example is the hardening of five discrete tracks inside a bore surface of a power steering housing (Hick, 1983) Very little is written about the improvement of fatigue properties. In a study, smooth 7 mm diameter rotating beam fatigue specimens were hardened over the entire cylindrical surface by a spiral track. The utmost µm melted and the hardened zone below was about 100 µm deep. The fatigue limit was raised by 30%. However this is a rather unrealistic use of laser hardening. For fatigue improvement one would rather think of hardening notches or fillets.

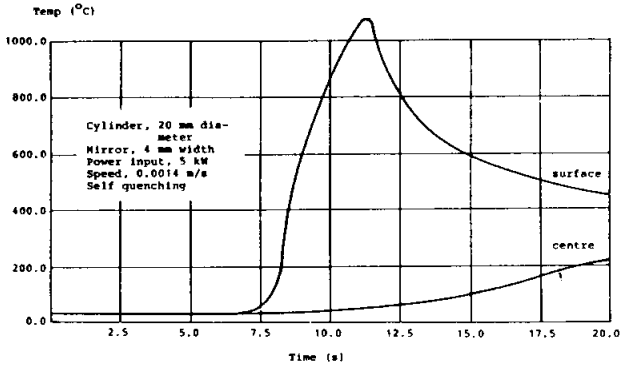

Fig. 10. Calculated temperatures in the centre and at the surface during laser hardening of a 20 mm diameter cylinder moved with 0.0014 m s^{-1} through a ring mirror with 4 mm axial length. Laser power is 5 kW and self quenching (Melander et al., 1984).

ELECTRON BEAM HARDENING

Electron beam hardening and laser hardening have much in common and several good reviews are available (Hick, 1983; ASM, 1981). In electron beam hardening a concentrated electron beam heats the surface of the workpiece to the austenitic range for a short while. The surface is then cooled by self-quenching and martensite is formed. The whole process operates in vacuum. The high energy electrons penetrate a few hundreds of a µm of the surface layer of the workpiece and no coating is needed for the absorption. The power output is larger than for lasers, usually in the range 30-60 kW but equipment up to 150 kW exists. As the electron beam is electrically charged it can easily be deflected by coils and made to form intricate scanning patterns on the surface. The beam diameter can be varied by focusing and is typically about 3 mm. By scanning and by defocusing the effective power density can be controlled to a few kW cm^{-2}, suitable for hardening.

The electron beam process is suitable for localized hardening like the laser process. The hardness depths obtainable is below 2-2.5 mm. As self-quenching is used larger depths require larger workpiece thickness.

The same types of steels and irons can be hardened by electron beams as by lasers. Electron beam hardening has not been studied so extensively as laser hardening so information about temperature cycles, microstructures and residual stresses is more scarce than for laser hardening. However, many of the findings about laser hardened structures probably also hold for electron beam hardening.

CARBURIZING AND CARBONITRIDING

There is extensive literature on carburizing and carbonitriding and several good overview descriptions of the process (ASM, 1981; Thelning, 1984) and the material properties (Parrish, 1976a, 1976b, 1976c, 1976d, 1977). In carburizing and carbonitriding carbon and carbon plus nitrogen respectively are taken up by the steel surface usually in a gas atmosphere at 850-1050°C to a depth between a few tenths of a millimeter and a few millimeters and then quenched in oil, a water solution or a polymer quenchant. This results in a structure of martensite with varying amounts of retained austenite at the surface and bainite and/or ferrite plus pearlite in the core. The coarseness of the structure is determined by the austenite grain size before quenching. Occasionally internal oxidation can be found at the very surface, sometimes accompanied by a pearlitic surface layer. The condition of the material is also characterized by the carbon and nitrogen profiles, the hardness and the residual stress distribution.

The developments of the process in the last few years has been driven by the increased cost of energy and hydrocarbon gases and by the new possibilities to control and automate the process given by improved gas sensors and micro-computers. In conventional gas carburizing, propane or natural gas has been used to generate endogas in a gas generator. The endogas is fed into the furnace and its carbon potential is monitored with infrared or dew-point instruments and adjusted by addition of small amounts of propane. In carbonitriding a certain amount of ammonia is added as well. The reactions in these processes have been studied in depth and computer models have been developed, see for instance Slycke (1981a, 1981b). A further development is to use nitrogen as a carrier gas and add air and natural gas or methanol directly into the furnace. It eliminates the need for gas generators and saves hydrocarbon gases (Chandler, 1984; Slycke, 1982).

The so-called oxygen probe has replaced infrared instruments, and microcomputers permit the use of more complicated process cycles with, for instance, boost and diffusion steps to speed up the process. Another way to speed up the process has been to increase the austenitising temperature from typically 900-925°C to 950-1000°C. This is possible by using fine grain treated steels specially designed for higher temperatures to avoid ausenite grain growth.

Much effort has also been made lately to understand the factors that affect the quenching process (Monroe, 1983; Thelning, 1983; Moreaux, 1980) in order to control it better. Thus all the stages in the carburizing/carbonitriding process can be better controlled and the resulting materials properties achieved to closer tolerances than before.

The progress of the phase transformation has been studied with computer modelling (Ericsson, 1982, 1984; Hildenwall, 1978; Burnett, 1981). Figure 11 shows how the austenite transforms in a 40 mm thick very wide plate quenched in oil from 850°C. The surface carbon content is 0.8% and the core carbon content 0.2% at 1 mm below the surface. The transformation starts well into the case because the transformation is delayed at the surface due to the decreased M_s there. The surface transforms later than the core due to the M_s effect and increased hardenability with high C-content.

For a 17 mm diameter cylinder with the surface carbon conten 0.8%, and the core carbon content 0.18% 1.5 mm below the surface, the bainite and martensite contents in the centre and at the surface are plotted as a function of time in Fig. 12. Figure 13 shows the corresponding residual stress values. During the first 7 s the stress distribution is of thermal character. The proeutectoid ferrite then starts to form at an intermediate depth (not shown here) which pushes both the surface and centre stress in the tensile direction. After 10 s bainite starts to form in the centre and the centre stress moves in the

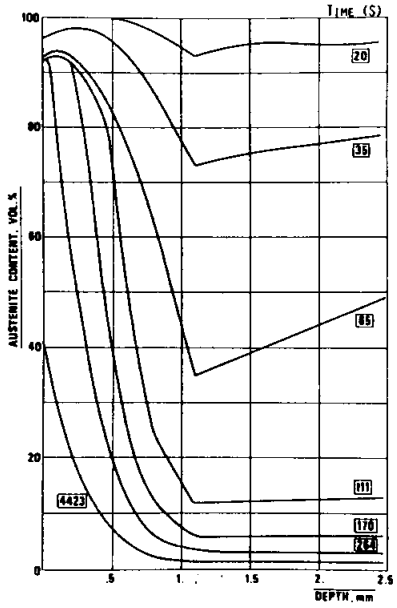

Fig. 11 Retained austenite content plotted against depth after various times from the beginning of the quenching of carburized SAE 1321 (C_s = 0.8% C, total case depth = 1 mm).

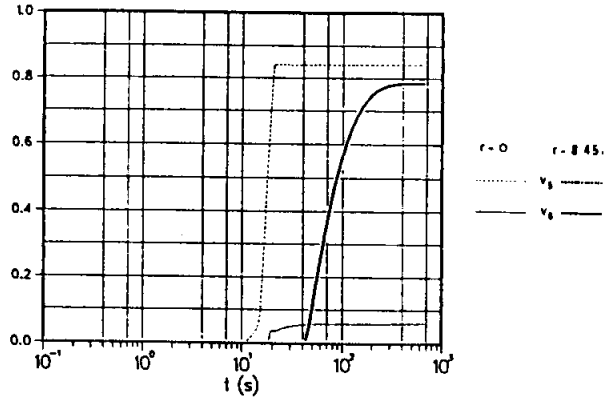

Fig. 12. Volume fractions of bainite, k = 5, and martensite, k = 6, for the central part and the surface of a cylinder (Ericsson, 1984).

compressive direction. After 12 s martensite and bainite start to form at the case/core interface (1.3 mm below the surface) moving the centre stress in the tensile direction, until the formation of bainite starts in the centre. After 19 s formation of martensite in the centre pushes the centre stress in the

compressive direction. After about 20 s the stress distribution is controlled by the transformation of the case. The last part to transform is the surface (after 40 s) and the martensite formation of the surface drastically pushes the surface stress to large compressive values. Figure 14 shows the complete stress distribution at selected time instances in the same specimen as Figs. 12, 13. The final distribution has a marked tensile peak below the case and a slight compressive stress in the centre. The final phase distribution is shown in Fig. 15. An analysis based on many calculations indicated that the maximum compressive stress for a certain carbon profile increased with increased cylinder diameter and that for a certain diameter it decreased with increased carburizing depth.

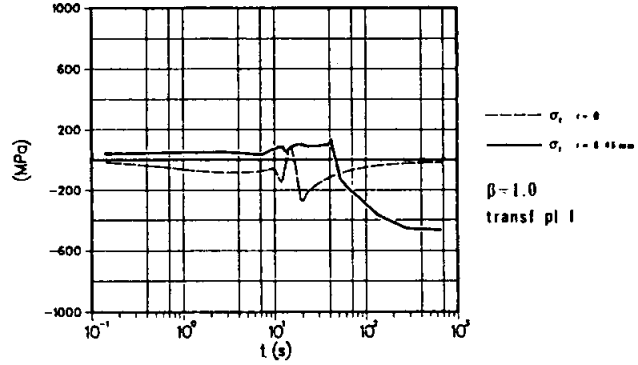

Fig. 13. Axial stress as a function of time for the central part and the surface of the same cylinder as in Fig. 11.

The maxinum compressive stress was thus obtained for a large diameter (30 mm) and a thin carbon profile (0.7 mm) (Ericsson, 1984).

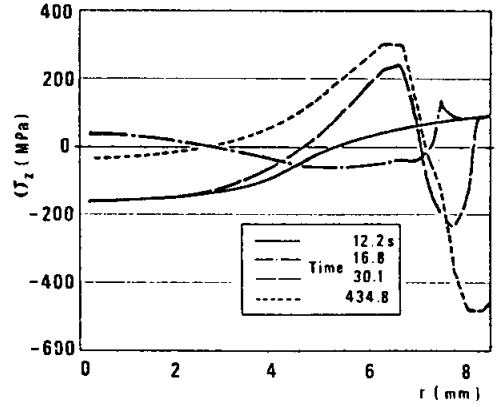

Fig. 14. Calculated axial stress for 12.2, 16.8, 30.1 and 434.8 s after the start of the quenching (Ericsson, 1984).

Calculations of residual stresses in more realistic parts have also been carried out for straight gears and the maximum of the compressive stress is found in the root and a little below the tip of a gear tooth (Inoue, 1984).

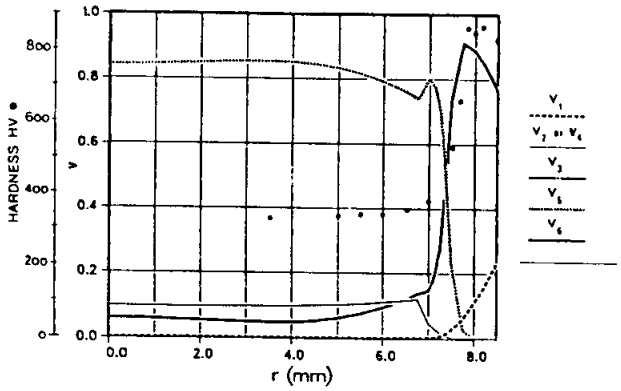

Fig. 15. Volume fractions of austenite, k = 1, ferrite, k = 2, bainite, k = 5, and martensite k=6, together with measured hardness values for the same cylinder as in Fig. 11.

The mechanical properties such as fatigue, contact fatigue and impact fracture of carburized materials have been extensively studied over the years. Several good review papers exist (Parrish 1976a, 1976b, 1976c, 1976d, 1977) and a recent book gives many aspects of the problem (Diesburg, 1984). An earlier extensive work should also be mentioned (ASM, 1957).

Usually the mechanical properties are discussed in terms of case depth, surface hardness, core hardness, surface carbon and nitrogen contents, retained austenite content, austenite grain size, surface oxidation and residual stresses.

A few rather definite statements can be made. Bending fatigue properties are impared by surface oxidation, sub-zero treatment (to transform retained austenite to martensite) and coarse austenite grain size (>ASTM 5); contact fatigue properties are improved by high retained austenite content.

The effect of retained austenite on bending fatigue is still very unclear. It has been claimed that it is beneficial (Brandis, 1984; Landgraf, 1975) or that it is detrimental (Beumelburg, 1974). The problem, as so often with carburized steel, is that it is not possible to vary the retained austenite content without changing other factors like surface carbon content, steel analysis, hardening temperature etc.

The bending fatigue properties of carburized/carbonitrided steel are usually discussed with the help of a "Woodvine analysis" (ASM, 1957) (first suggested in 1924). The stress is plotted along the y-axis and the distance from the surface on the x-axis. The fatigue strength profile is derived from the hardness profile using an empirical fatigue limit-hardness curve.

The fatigue strength thus calculated and the applied (elastic) stress are drawn in the diagram. The fatigue strength is corrected with the residual stress. This type of diagram can qualitatively describe the effect of case depth, hardness profile and residual stress on the fatigue limit and the phenomenon of sub-surface fatigue crack initation (ASM, 1957; Hopkins, 1976). It has been refined to include the residual microstress as well as the residual macrostress (Mittemeijer, 1983). Recently a much more refined analysis of the condition for fatigue crack propagation has been presented, based on fracture mechanics (Kim, 1984). The treatment starts to analyse static bending fracture before

going on to fatigue fracture. A load-displacement diagram is derived considering a fracture toughness that varies with the depth under the surface. The maximum load for a fracture bend test is found to occur for a certain crack length, not for zero crack length, to decrease with increased case depth and to increase with increased core fracture toughness (Fig. 16).

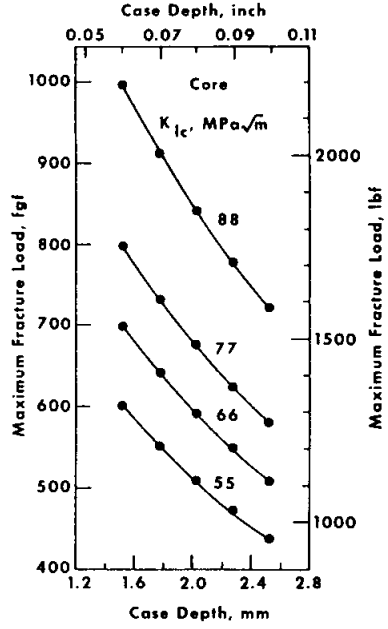

Fig. 16. Influence of case depth and core fracture toughness on maximum fracture load for tooth specimen (Kim, 1984).

A stress intensity factor due to the residual stress is then derived, which is negative if the residual stresses are compressive. To propagate a fatigue crack the difference between the applied fatigue load stress intensity and the residual stress intensity has to exceed the threshold value for fatigue crack propagation. The analysis predicts that in realistic instances cracks have to be larger than a tenth of a milimeter to propagate, and the situation may occur that a growing cracks stops (Fig. 17). The analysis does not consider subsurface crack propagation but it should be possible to extend the theory to cover this situation.

COMPARISON OF METHODS

The relative merits (+) and drawbacks (-) of thermal and thermo- chemical austenitic hardening processes can be summarized as follows (Carlsson, 1980; Hick, 1983).

All Thermal Hardening Processes

+ Short process time
+ Very suitable for localized hardening
+ Clean processes that can be integrated in a manufacturing line
- The prior steel microstructure influences the result

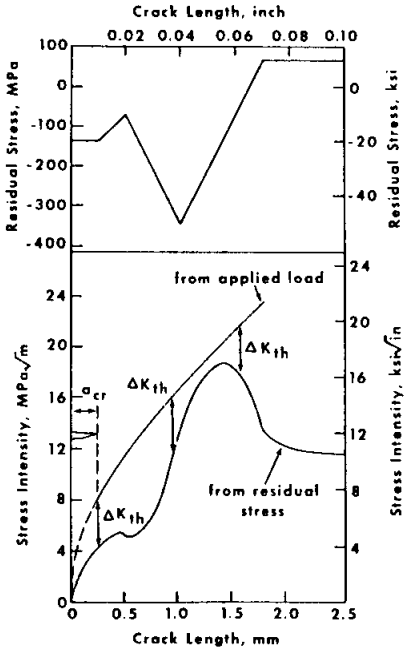

Fig. 17. Stress intensity change due to a residual stress field typical in carburized steel (Kim, 1984).

Induction Hardening

+ Large case depths are obtainable
+ Energy consumption is low
- External cooling required

Laser- and Electron Beam Hardening

+ Steels with lower carbon content than for induction hardening can be hardened
+ No external cooling needed
+ The heating source can easily be moved over the surface, especially true of the electron beam
+ No hardening distortions
- Only small hardening depths feasible
- Vacuum chamber needed (electron beam hardening)
- Coating of the steel surface needed (laser hardening)
- High investment cost

Thermochemical Hardening Processes (Carburizing/Carbonitriding)

+ Large surface can be hardened
+ Large case depths are obtainable
+ High surface hardness
- Hardening distortions occur
- Relatively long process time
- High energy consumption

The methods are interchangable for some applications but not for others. Carburizing/carbonitriding compete with induction hardening for many applications involving fatigue and there is a trend to increased use of induction hardening. Laser- and electron beam hardening are not yet much used. They are especially advantageous for wear problems and for hardening of very small areas. They either compete with high-frequency induction hardening or open up new hardening applications. As these processes are the newest more remains to study about resulting material properties and suitable applications for them than for induction hardening or carburizing. We will certainly see many papers dealing with laser- and electron beam hardening in Advances in Surface Treatments.

REFERENCES

American Society for Metals, (1957). Fatigue Durability of Carburized Steel, ASM, Cleveland.

American Society for Metals, (1981). Metals Handbook, 9th edn, Vol. 4. Heat Treating.

Ashby, M.F., K. E. Easterling, and W-B Li (1984). Modeling the laser transformation hardening of steel. Acta Metall. To be published.

Ashby, M. F. and K. E. Easterling (1984). The transformation hardening of steel surfaces by laser beams. Acta Metall. To be published.

Atlas zur Warmebehandlung der Stahle (1973). Band 3, Verlag Stahleisen, Dusseldorf.

Beumelburg, W. (1974). Das Erhalten von einsatzgehärteten Proben mit verschiedenen Oberflächenzustanden and Randkohlenstoffgehalten im Umlauf biege-, statischen Biege- und Schlagbiegeversuch. Dissertation, Karlsruhe University

Bobart, G. F. (1982). Innovative induction heat treat systems. J Heat Treating, 2, 351-358

Brandis, H. and W. Schmidt (1984). Contribution of the effect of retained austenite on the measured properties of case-hardened steel. In D. E. Diesburg (ed.) Case-hardened Steel: Microstructure and Residual Stress Effects, Metal Society of AIME, Warrendale, pp. 189-210.

Burnett, J. A. (1981). Prediction of stresses generated during the heat treating of case carburized parts. In L. J. Vange Walle (ed.) Residual Stress for Designers and Metallurgists. ASM, Metals Park, pp. 51-70.

Carlsson, K-O. (1980). Surface Hardening with Laser and Electron Beam. IVF-resultat 800623, Mekan, Stockholm.

Chandler, H. E. (1984). Heat treating/processing technology in 1990. Metal Progress, 126, 59-70

Chatterjee-Fischer, R., R. Rothe, and R. Becker (1984). Überblick über das Härten mit dem Laserstrahl. Härterei-Technische Mitt., 39, 91-98.

Courtney, C., and W. M. Steen (1981). The surface heat treatment of En 8 steel using a 2 kW CO_2 laser. In Source Book on Applications of Laser in Metal-working. ASM, Metals Park, pp. 195-208.

Diesburg, D.E. (ed.) (1984). Case-hardened Steels. Micro-structural and Residual Stress Effects. Metal Society of AIME, Warrendale.

Ericsson, T., and B. Hildenwall (1982). Thermal and transformation stresses. In E. Kula and V. Weiss (eds.), Residual Stress and Stress Relaxation, Plenum, New York.

Ericsson, T., S. Sjöström, M. Knuuttila, and B Hildenwall (1984). Predicting residual stresses in cases. In D.E. Diesburg (ed.) Case-Hardened Steels: Microstructural and Residual Stress Effects. Metal Society of AIME, Warrendale, pp. 113-140.

Godfrey, D.J, A. C. Hill, and C. Hill (1981). A computer model for pulsed laser heating of device structures. Solid-State Science and Techn., 1798-1803.

Hick, A. J. (1983). Rapid surface heat treatments: A review of laser and electron beam hardening. Heat Treatment of Metals, 10, 3-11.

Hopkins, R. B. (1976). Estimating strength properties of heat treated parts. Soc. Automotive Eng., 760409, Warrendale.

Hildenwall, B., and T Ericsson (1978). Prediction of residual stresses in case-hardening steels. In Doane and J. Kirkaldy (eds.) Hardenability Concepts with Application to Steel. Metal Society of AIME, Warrendale.

Inoue, T., Z-G. Wang, and T. Yamaguchi (1984). Quenching stresses of carburized steel gear considering phase transformations. In E. Attebo and T. Ericsson (eds.) Calculation of Internal Stresses in Heat Treatment of Metallic Materials, Linköping University, pp. 387-398.

Ishii, K., M. Iwamoto, T. Shiraiwa, and Y. Sakamoto (1969). Residual stress in the induction hardened surface of steel. Soc. Automotive Eng., 690472, Warrendale.

Kawasumi,. H. (1981). Metal surface hardening CO_2 laser. In Source Book on Applications of the laser in Metalworking, ASM, Metals Park, pp. 185-194.

Kim, C. (1984). Fracture of case-hardened steels and residual stress effects. In D. E. Diesburg (ed.) Case-hardened Steels: Microstructural and Residual Stress Effects. Metal Society of AIME, Warrendale, pp. 59-88.

Kou, S., and D.K. Sun (1983). Heat flow during the transformation hardening of cylindrical bodies. Met. Trans., 14A, 1859-1867.

Melander, M. (1982). The single shot induction hardening cycle: A computational approach. Linköping Studies in Science and Technology, LiU-Tek-Lic-1982:5, Linköping.

Melander, R. (1983). Computer calculations of residual stresses due to induction hardening. In E. Macherauch and V. Hauk (eds.) Eigenspannungen. Enstehung-Messung-Bewertung, Deutsche Gesellschaft für Metallkunde, Oberursel, pp. 309-328.

Melander, M. (1984). Computer predictions of progressive induction hardening of cylindrical geometries. In E. Attebo and T. Ericsson (eds.) Calculations of Internal Stresses in Heat Treatment of Metallic Materials. Linköping University, Linköping.

Melander, M., Yao Shan Chang, and T. Ericsson (1984). Theoretical and experimental study of induction and laser hardening. In Heat Treatment Shanghai '83. Metals Society, London.

Metals Society, (1972). Heat Treatment '71. Metals Society, London.

Metals Society, (1974). Heat Treatment '73. Metals Society, London.

Metals Society, (1977). Heat Treatment '76. Metals Society, London.

Metals Society, (1980). Heat Treatment '79. Metals Society, London.

Metals Society, (1982). Heat Treatment '81. Metals Society, London.

Metals Society, (1984). Heat Treatment '83. Metals Society, London.

Metals Society, (1985). Heat Treatment '84. Metals Society, London.

Molian, P. A. (1981). On the presence of retained austenite in laser transformation hardened low alloy steel. Scripta Metall. 15, 1101-1104

Moreaux, F., A. Simon, and G. Beck (1980). Simultaneous increases of hardness depth and decrease of quench defects in steel parts by adapting the cooling process. 1st International Conference on Heat Treatment of Materials, Detroit.

Monroe, R. W., and C. E. Bates (1983). Evaluating quenchants and facilities for hardening steel. J. Heat Treating, 3. 83-99.

Mittemeijer, E. J. (1983). Fatigue of case-hardened steels: Role of residual macro- and microstresses. J. Heat Treating, 3, 114-119.

Parrish, G. (1976a). Heat Treatment of Metals, 3, 6-11

Parrish, G. (1976b). Heat Treatment of Metals, 3, 49-53

Parrish, G. (1976c). Heat Treatment of Metals, 3, 73-78

Parrish, G. (1976d). Heat Treatment of Metals, 3, 101-109

Parrish, G. (1977). Heat Treatment of Metals, 4, 17-27

Reinke, F. H., and W. H. Gowan (1978). Recent developments in induction hardening. Heat Treatments of Metals, 5, 39-45.

Slycke, J., and T. Ericsson (1981a). A study of reactions occurring during the carbonitriding process. Part I. J. Heat Treating, 2,

Slycke, J., and T. Ericsson (1981b). A study of reactions occurring during the carbonitriding process. Part II. J. Heat Treating, 2,

Slycke, J. (1982). Aufkohlung in synthetischen Ofenatmosphären. Harterei-Techn. Mitt., 121-129.

Thelning, K-E. (1983). New aspects on the appraisal of the cooling process during hardening of steel. J. Heat Treating, 3, 100-107.

Thelning, K-E. (1984). Steel and Its Heat Treatments, 2nd edn. Buttersworths, London.